Arrest of Domain Coarsening via Antiperiodic Regimes in Delay Systems

J. Javaloyes,[1] T. Ackemann,[2] and A. Hurtado[3]
[1]Departament de Física, Universitat de les Illes Baleares, C/ Valldemossa km 7.5, 07122 Mallorca, Spain
[2]SUPA and Department of Physics, University of Strathclyde, John Anderson Building, 107 Rottenrow, Glasgow G4 0NG, United Kingdom
[3]Institute of Photonics, SUPA and Department of Physics, University of Strathclyde, Technology and Innovation Centre, 99 George Street, Glasgow G1 1RD, United Kingdom
(Received 10 March 2015; published 10 November 2015)

Motionless domain walls representing connecting temporal or spatial orbits typically exist only for very specific parameters, around the so-called Maxwell point. This report introduces a novel mechanism for stabilizing temporal domain walls away from this peculiar equilibrium, opening up new possibilities to encode information in dynamical systems. It is based on antiperiodic regimes in a delayed system close to a bistable situation, leading to a cancellation of the average drift velocity. The results are demonstrated in a normal form model and experimentally in a laser with optical injection and delayed feedback.

DOI: 10.1103/PhysRevLett.115.203901 PACS numbers: 42.65.Sf, 02.30.Ks, 05.45.-a

Spatially extended nonlinear systems often admit multiple coexisting stable states, and the dynamical properties of the fronts connecting them are fundamental in the understanding of pattern formation and localized structures (LS). These dissipative objects [1–11] occur in many natural and laboratory systems and are characterized by a correlation range much shorter than the size of the domain, making them individually addressable. Localized structures due to a front between a homogeneous and a cellular state are intrinsically stable [12–14], as the pattern oscillations stabilize the position of the front against small perturbations. In contrast, fronts between homogeneous states are typically stable only for very specific parameters and lead otherwise to a coarsening.

In this Letter, we discuss a robust mechanism for the stabilization of fronts between homogeneous states based on a generic property of time delayed systems having no equivalent in spatially extended systems. We show that structures occurring within a time delay can be stabilized by a flip inversion occurring at each cycle, thus allowing the stabilization of self-localized temporal domains. The case of equispaced domain walls reduces to the so-called square waves [15,16]. This has not only relevance for the fundamentals of the dynamics of delayed systems, but also meets recent interest in temporal LS realized in photonics [17–23]. Because of their intrinsically fast dynamics, the possibility to use LS as bits for information processing was addressed early in nonlinear optics [24–26]. Interesting results were achieved for spatial solitons in semiconductor microcavities [27–29], although it turned out that spatial disorder limits parallelism and control [30,31], motivating further studies into temporal LS.

As indicated, in the simple case of a unidimensional bistable system with a single dynamical variable $\psi(x,t)$, the stable coexistence between two homogeneous phases is merely achieved for a single value of the parameters, the so-called Maxwell point. Here a domain wall separating the two states would be motionless. Yet, such a regime possesses little experimental significance since any deviation of the control parameter or any symmetry breaking effect implies that one of the two bistable phases will eventually invade the other in a way reminiscent of nucleation bubbles in first order phase transitions.

In recent years, building on the strong analogies between spatial and delayed systems [32–34], a similar symmetry breaking induced coarsening dynamics was shown to occur in delayed bistable systems [35,36]. The ability to control the motion of these walls would have significant implications, as for instance to encode and process information with a fast nonlinear delayed system. Motivated by this idea, the pinning of domain walls was recently demonstrated via an external temporal modulation [37]. Departing from the analogies with spatial systems, we demonstrate in contrast a stabilization mechanism based not upon a fast active modulation, but upon a slow, self-induced dynamics. We envision the use of a lesser known property of delayed systems: their ability to generate antiperiodic output, i.e., temporal traces getting inverted after each time delay τ, thereby inducing an effective periodicity 2τ.

While this effect was studied theoretically in Refs. [15,16,38] and square waves were demonstrated experimentally in several optical [39,40] and optoelectronic systems [41], we demonstrate in this Letter how this generic property of antiperiodicity can be harnessed to create robust motionless domain walls and prevent the coarsening phenomenon. This allows us to store information even far from the Maxwell point and/or in the absence of bistability. Such an idea has no equivalent in bona fide spatial systems since the antiperiodicity would actually correspond to a space defined over a Möbius strip. We evidence experimentally and theoretically stable domains in an injected semiconductor laser with delayed feedback that are insensitive to symmetry breaking and exist beyond the bistability regime.

We base our analysis on the normal form of the imperfect pitchfork bifurcation modified by the inclusion of a linear delayed contribution

$$\varepsilon \frac{d\Psi}{dt} = \mu\Psi + \beta\Psi^2 - \Psi^3 + \eta\Psi(t-1). \quad (1)$$

In Eq. (1), the parameter μ controls the bistability, β represents the symmetry breaking, and η is the amplitude of the time delayed feedback. The temporal scale is normalized by the time delay τ. We study the limit of long delays $\tau \to \infty$, and define a smallness parameter $\varepsilon = 1/\tau$ making apparent the singular nature of Eq. (1). Delay differential equations possess in the long delay limit an eigenvalue spectrum that can be divided in two parts, see for instance Ref. [42] and references therein. A quasicontinuous branch stems from the influence of the delayed contribution while a discrete spectrum is generated by the instantaneous linear terms. We are interested in the regimes where a portion of the quasicontinuous branch may become unstable giving rise to smooth dynamics. We set $\mu < 0$ ensuring the stability of the discrete spectrum. When $\varepsilon \to 0$, the left-hand side of Eq. (1) can be assumed, as a first approximation, to vanish. Such an approach is enlightening as one finds a functional mapping governing the evolution of the small deviations from the trivial solution $\Psi = 0$ as

$$\Psi(t) = -\kappa\Psi(t-1) \quad (2)$$

with $\kappa = \eta\mu^{-1}$. Because of the infinite dimensionality of delay differential equations, an initial condition must be given as a function defined over an interval equal to the delay. If $|\kappa| < 1$, any initial condition slowly decays from one round-trip to the next and the steady state $\Psi(t) = 0$ is asymptotically stable. Yet, for $|\kappa| > 1$, the trivial solution may bifurcate via two widely different scenarios. If $\kappa < -1$, the temporal profile evolves regularly from one round-trip to the next while for $\kappa > 1$, the profile gets inverted at each round-trip signaling the onset of a period-2 ($P2$) regime.

The slowly evolving dynamics of the temporal profile can be better understood and visualized via the spatiotemporal equivalence between delayed and spatially extended systems [16,32–34,42]. We define the deviation from the two bifurcation points $\mu = \eta\kappa^{-1}$ with $\kappa = \pm 1$ as $\mu = a + \varepsilon^2 a_1$ and $\eta = a\kappa + b_1\varepsilon^2$ and, as detailed in Ref. [42], inserting a multiple time scale expansion in Eq. (1) for both the temporal derivative and the delayed term, and defining $\Psi = \varepsilon\psi + \mathcal{O}(\varepsilon^2)$, one obtains the following equivalent partial differential equation as a third order solvability condition

$$\frac{\partial\psi}{\partial n} = p\psi + \frac{\beta}{a}\psi^2 + \frac{\psi^3}{a} + \frac{1}{2a^2}\frac{\partial^2\psi}{\partial x^2} \quad (3)$$

with $p = -(a_1 - \kappa b_1)/a$. Although strictly valid in the vicinity of the bifurcation points, such normal forms are known to have a wider domain of validity, see the discussion before Eq. (8a) in Ref. [16]. In Eq. (3), the spatial coordinate (x) must be understood as a local time coordinate within the round-trip while the slow time (n) represents the evolution of the temporal profile from one round-trip to the next. Besides, we factored out a drift velocity defined as $v = a^{-1}$ as in Refs. [23,33], representing the small deviation of the period with respect to the time delay. Equation (3) must be complemented by a boundary condition that reads

$$\psi(x+1, n) = -\kappa\psi(x, n) \quad (4)$$

and defines, as in Eq. (2), whether or not the solution gets inverted from one round-trip to the next. For $\beta = 0$ and $a < 0$, the heteroclinic orbits of Eq. (3) read $K_\pm(x) = \pm\sqrt{|a|p}\tanh(|a|\sqrt{p}x)$, where the $\pm$ stands for the upward and downward domains walls. In deriving Eq. (1) we assumed that the symmetry breaking term β scales as ε to enter as a perturbation of the solvability condition. Yet, although small, β has a deep impact upon the dynamics.

We depict in Fig. 1(a) an initial condition for Eq. (1) composed of an arbitrary succession of domains with values corresponding to the plateaus of the $P1$ or of the $P2$ regimes. In the $P1$ case ($\kappa = -1$) as visible in Figs. 1(b) and 1(c), this multiplateau pattern relaxes in a finite time to the upper (lower) value when $\beta < 0$ ($\beta > 0$). Such a coarsening scenario is very general and it is preserved quite far from

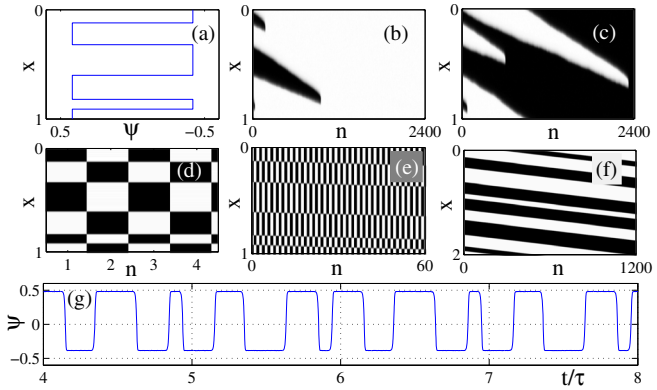

FIG. 1 (color online). Illustration of dynamics in space-time diagrams. These space-time diagrams are folded over a time $T = \tau + |\eta|^{-1}$. (a) Temporal pattern imposed as an initial condition. The $P1$ regime where $\kappa = -1$ leads to the coarsening dynamics of the temporal time trace depicted in (b) and (c) towards the high and low states when $\beta = -10^{-2}$ (b) and $\beta = 10^{-2}$ (c), respectively. Other parameters are $\tau = 10^3$, $\eta = 5 \times 10^{-2}$, and $\mu = 2.5 \times 10^{-2}$, or equivalently $a = -5 \times 10^{-2}$, $b_1 = 0$, and $a_1 = 7.5 \times 10^4$. The $P2$ regime where $\kappa = 1$ induces the inversion of the initial condition at each round-trip as exemplified by the checkerboard pattern in (d). It does not coarsen over longer time scales even for very large values of the asymmetry $\beta = 0.1$. The time trace is folded over times T in (e) and also $2T$ in (f) for clarity. Parameters are $\eta = -0.2$ and $\mu = -2.5 \times 10^{-2}$, or equivalently $a = -0.2$, $b_1 = 0$, and $a_1 = 17.25 \times 10^4$. The temporal profile is represented in (g). Notice the large values of a_1, signaling that Eq. (3) remains qualitatively valid far from the bifurcation points.

the bifurcation condition $\mu = -\eta$, and even when the discrete spectrum is also unstable, i.e., with $\mu > 0$. A multidomain solution that verifies Eqs. (3) and (4) can be written as

$$\psi(x,n) = K_+(x - x_0^+) + K_-(x - x_1^-) + \cdots + K_-(x - x_n^-) - \sqrt{|a|p} \quad (5)$$

with $\{x_n^\pm\}$ the ordered collection of the coordinates of the upward and downward kinks. For $|\beta| \ll 1$, a variational approach is justified [43], and we insert an ansatz as $\psi(x,s) \sim K_\pm[x - x_\pm(s)]$. By multiplying Eq. (3) by $\partial_x K_\pm$ and integrating over the spatial coordinate, we find the effective equation for the motion of an isolated wall as

$$\frac{dx_i^\pm}{dn} = \mp \frac{\beta}{2a\sqrt{|a|}}, \quad (6)$$

demonstrating that the symmetry breaking term β induces a splitting of the velocity of domain walls of opposed "charge", which will eventually collide. Notice that the value of the drift can also be found searching for heteroclinic solutions of Eq. (1) as in Ref. [35]. Both methods neglect the short range, exponentially decreasing interactions between nearby walls that are known to be attractive [16,38,43]. This can lead for $\beta < 0$ to a steady state, which is however unstable and cannot prevent the eventual collision and coarsening. Hence, one may conclude that it is impossible to store information in a scalar delayed system as any symmetry breaking nonlinearity leads to a coarsening of the information.

We now demonstrate how a completely different regime can be obtained exploiting the antiperiodic solutions of Eq. (1) achieved by simply setting $\eta < 0$ to access the regime where $\kappa = 1$. We stress that here, since $\mu < 0$, bistability is lost and the only steady solution is $\Psi = 0$. Surprisingly, stable domains with well defined plateaus can be obtained even in this regime, although the time trace gets inverted every round-trip, thereby inducing a periodicity close to twice the delay value 2τ, see Figs. 1(d)–1(g). Although the solution inversion is interesting in its own right, such a behavior can be deduced intuitively from the singular mapping (2) setting $\kappa = 1$. The striking result is that the domain walls remain motionless, even for large β values, see Figs. 1(d) and 1(e), where the checkerboard pattern visually disappears leaving only visible the transitions. We verified this robustness with other kinds of symmetry breaking terms, e.g., $\gamma_m \Psi^m$ with $m = 0$ and $m = 4$. One can still construct approximate analytic solutions of Eq. (3) where an upward or a downward kink must be complemented by an opposed kink at a spatial distance $x = 1$ in order to fulfill the antiperiodic boundary condition (4). A similar variational approach allows us to find the effective equation of motion of an isolated wall

$$\frac{dx_i}{dn} \sim \beta \int_0^2 (\partial_x K_+ + \partial_x K_-)(K_+ + K_-)^2 dx = 0. \quad (7)$$

In other words, by inverting at each round-trip, the walls experience opposed drift velocities that cancel out, explaining why similar results can be found for other kinds of symmetry breaking nonlinearities. It was also demonstrated in Ref. [16] that the quadratic term cancels out of Eq. (3) even if it is large, see Eqs. (A.17) and (A.18) in Appendix A of Ref. [16] for details. Higher order nonlinearities in Eq. (1) potentially as large as $\gamma_m \sim \varepsilon^{3-m}$ may enter Eq. (3), but would cancel out similarly in Eq. (7). We conclude that $P2$ delayed systems are robust candidates for information storing as they are impervious to most experimental imperfections leading to a coarsening.

For a demonstration, we study the case of an injected semiconductor laser below threshold subject to optical feedback, as domain stabilization in telecommunication lasers is very interesting also from an applicative point of view. Close to, yet below, threshold and in the limit of weak optical feedback, weak optical injection, small detuning, and large delay, one can reduce the standard single-mode rate equations of the semiconductor laser to the following delayed Ginzburg-Landau equation

$$\dot{E} = (1 + i\alpha)(J - |E|^2)E + i\Delta E + Y + \tilde{\eta} e^{-i\Omega} E(t - \tau), \quad (8)$$

see, for instance, Ref. [23] for details. Here, J denotes the deviation from threshold of the bias current. The detuning between the frequency of the injection field ω_Y of amplitude Y (chosen real by definiteness) and the free running frequency of the laser scaled by the photon lifetime is Δ, while $\tilde{\eta}$ and $\Omega = \omega_Y \tau$ are the amplitude and phase of the delayed optical feedback, respectively. At steady state ($\dot{E} = 0$), the output power $|E|^2$ as a function of Y can present a bistable S-shape response for some parameters. We work close to the onset of bistability where the transition from low to high power has a sigmoid shape, see the blue line in Fig. 2(a).

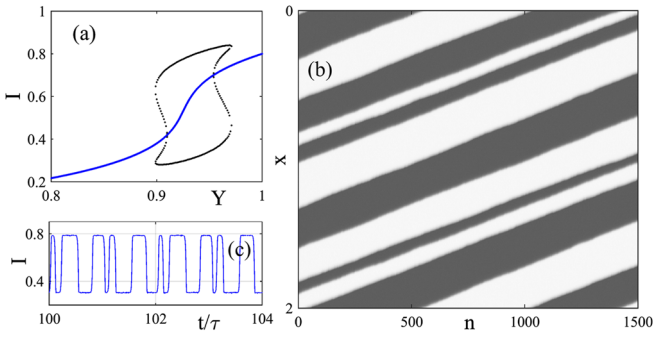

FIG. 2 (color online). (a) Nonlinear output intensity $I = |E|^2$ as a function of the injected field Y in blue. The black dots represents the amplitude of the upper and lower plateau in the $P2$ regime. The space-time diagram of the intensity in panel (b) is folded with a period $T = 2\tau + 0.1$ and shows the stability of the domain walls, even in the presence of noise, see also panel (c). Parameters are $\alpha = 2$, $J = -0.1$, $\Delta = 2.3$, $\tilde{\eta} = 0.1$, and $\Omega = \pi$.

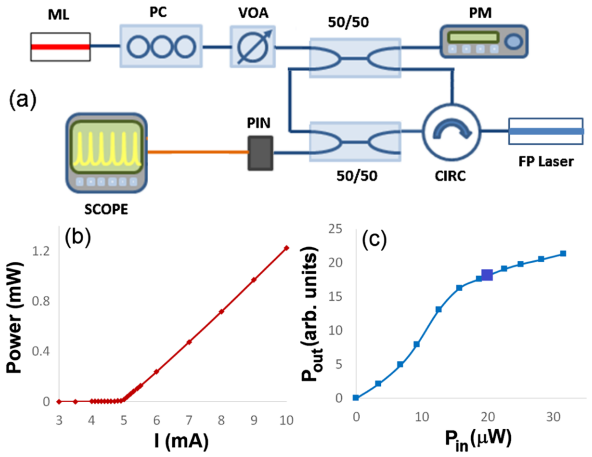

FIG. 3 (color online). (a) Experimental setup. ML, master laser; PC, polarization controller; VOA; variable optical attenuator; PM, power meter; FP, Fabry-Perot; CIRC, circulator; PIN, 12 GHz photodetector; SCOPE, 13 GHz oscilloscope. (b) LI curve of the SL at $T = 293$ K. (c) I/O power relationship of the SL under external injection with $\Delta f = -10$ GHz and $I = 4.85$ mA.

Assuming that a $P2$ solution evolves between two plateaus whose values are $E_{\pm}$, Eq. (8) yields a system of equations whose solution is represented by the black dots in Fig. 2(a). Such a diagram suggests that these $P2$ regimes are nascent from two saddle-node bifurcations of limit cycles and are also connected to the stationary solution (blue line) by two Andronov-Hopf bifurcations. However, these bifurcations are subcritical, meaning that the equivalent partial differential equation would certainly take the form of a subcritical cubic-quintic Ginzburg-Landau equation. Notice that for dynamical systems with a higher number of variables, as in Eq. (8), additional instabilities like the Eckhaus mechanism [44] may arise. Yet, Eq. (8) can be reduced to a single scalar delayed equation for the phase in the limit of weak feedback and injection using averaging methods [45]. We show indeed in Figs. 2(b) and 2(c) that this system is capable of storing patterns of domain walls.

The experimental setup is represented in Fig. 3. A 1310 nm Fabry-Perot laser [slave laser (SL)] as used in telecommunication systems is subject simultaneously to external optical injection and delayed feedback after a round-trip time $\tau = 65.4$ ns. The optically injected signal was generated with a tunable laser [master laser (ML)]. A polarization controller and a variable optical attenuator were, respectively, included after the ML to control its polarization state and optical power level. Figure 3(b) plots the light-current (LI) curve of the solitary SL, showing a threshold current of $I_{\mathrm{th}} = 4.92$ mA. Figure 3(c) depicts the SL's input or output power relationship when subject solely to external injection. The device was biased below threshold with a current of $I = 4.85$ mA (i.e., $I = 0.985 I_{\mathrm{th}}$) and an initial frequency detuning ($\Delta f = f_{\mathrm{inj}} - f_{\mathrm{FP}}$) equal to -10 GHz was set between the frequencies of the injected signal and the resonance frequency of one of the SL modes.

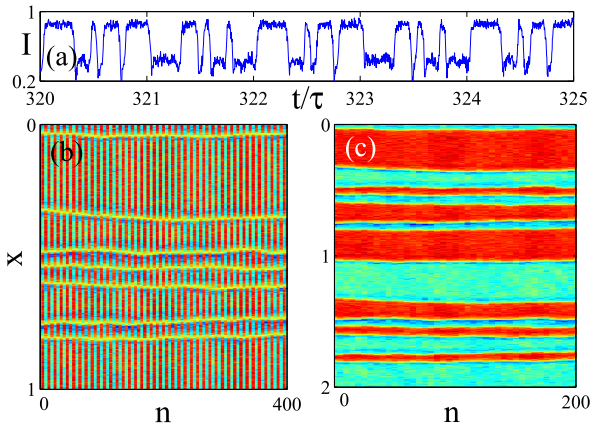

FIG. 4 (color online). Temporal trace of the laser intensity (a) and space-time diagram with folding parameter τ (b) and 2τ (c).

Figure 3(c) illustrates the achievement of a gradual nonlinear switching response as the injection strength is increased from 0 to 31.5 μW, in agreement with the results of Fig. 2(a).

The SL was subsequently subjected to simultaneous optical injection from the ML (input power $P_{\mathrm{inj}} = 20$ μW) and delayed feedback. In this situation the system was operated in the sigmoid range as indicated by the blue square in Fig. 3(c). The phase of the feedback can be changed by a small detuning of the injection field frequency. The large values of the time delay allow considering these two parameters to be independent.

Figure 4(a) plots the time trace over five round-trips (327 ns). Figure 4(a) shows that a temporal pattern, which is inverted every round-trip, is obtained at the device's output, in agreement with the predictions of Figs. 1(g) and 2(c). The equivalent space-time diagrams for the time series of Fig. 4(a) when the folding parameter is set approximately to τ and 2τ are plotted, respectively, in Figs. 4(b) and 4(c) over a time window of 400 round-trips (i.e., $\sim$26 μs). Figures 4(b) and 4(c) demonstrate the experimental achievement of antiperiodic dynamical regimes since peaks and troughs alternate every round-trip, see Fig. 4(b). More importantly, the results also demonstrate the formation of stable domains of arbitrary size. The existence of various noise sources in the system induces a slow drift of the walls as

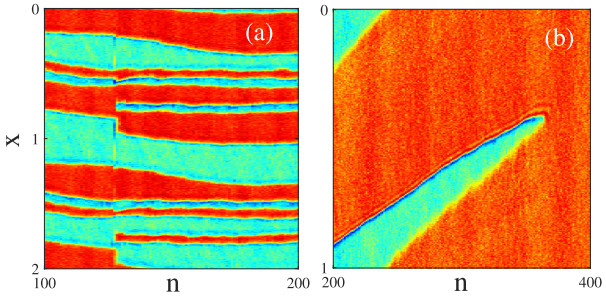

FIG. 5 (color online). Same as Fig. 4. A new pair of domain wall is nucleated at $n = 128$ in panel (a) and remains stable while for different parameters bistable phase coarsening occurs.

seen in Fig. 4(c), but not a coarsening if the walls remain at a sufficiently large distance, in good agreement with theory.

Of note, we observed the nucleation of domain wall pairs after the arrival of an electrical perturbation into the system as shown in Fig. 5(a) at $n = 128$. Additionally, a small change of the injection parameters allows us to observe in Fig. 5(b) the coarsening mechanism of the $P1$ solutions, as in Ref. [35].

In conclusion, we described in this Letter how a general property of delayed systems can be harnessed to prevent the domain coarsening in symmetry broken delayed systems, thereby allowing the storing of information. Such antiperiodicity has no equivalent in real spatially extended systems. We evidenced the existence of stable domains in the coherent output of a semiconductor laser with optical feedback. These results offer exciting prospects for the controllable encoding of information.

J. J. acknowledges a useful discussions with S. Balle as well as financial support from the Ramón y Cajal program and project RANGER (TEC2012-38864-C03-01). A. H. thanks Professor A. Kemp for lending the oscilloscope used in the experiments and acknowledges financial support from the Stratchlyde Chancellor's Fellowships Programme: Starter Grant (Ref 12431DP2425AOOO), Institute of Photonics, University of Strathclyde.

[1] S. Fauve and O. Thual, Solitary waves generated by subcritical instabilities in dissipative systems, Phys. Rev. Lett. **64**, 282 (1990).

[2] N. Akhmediev and A. Ankiewicz, *Dissipative Solitons, Lecture Notes in Physics* Vol. 661 (Springer, Berlin, 2005).

[3] N. Akhmediev and A. Ankiewicz, *Dissipative Solitons: From Optics to Biology and Medicine Series*, Lecture Notes in Physics Vol. 751 (Springer, Berlin, 2008).

[4] P. B. Umbanhowar, F. Melo, and H. L. Swinney, Localized excitations in a vertically vibrated granular layer, Nature (London) **382**, 793 (1996).

[5] Y. A. Astrov and H. G. Purwins, Plasma spots in a gas discharge system: birth, scattering and formation of molecules, Phys. Lett. A **283**, 349 (2001).

[6] Yu. Astrov, E. Ammelt, and H.-G. Purwins, Experimental evidence for zigzag instability of solitary stripes in a gas discharge system, Phys. Rev. Lett. **78**, 3129 (1997).

[7] F. J. Niedernostheide, M. Arps, R. Dohmen, H. Willebrand, and H. G. Purwins, Spatial and spatio-temporal patterns in pnpn semiconductor devices, Phys. Status Solidi B **172**, 249 (1992).

[8] K.-J. Lee, W. D. McCormick, J. Pearson, and H. L. Swinney, Experimental observation of self-replicating spots in a reaction-diffusion system, Nature (London) **369**, 215 (1994).

[9] J. Wu, R. Keolian, and I. Rudnick, Observation of a nonpropagating hydrodynamic soliton, Phys. Rev. Lett. **52**, 1421 (1984).

[10] E. Moses, J. Fineberg, and V. Steinberg, Multistability and confined traveling-wave patterns in a convecting binary mixture, Phys. Rev. A **35**, 2757 (1987).

[11] L. A. Lugiato, Introduction to the feature section on cavity solitons: An overview, IEEE J. Quantum Electron. **39**, 193 (2003).

[12] Y. Pomeau, Front motion, metastability and subcritical bifurcations in hydrodynamics, Physica (Amsterdam) **23D**, 3 (1986).

[13] P. Coullet, C. Riera, and C. Tresser, Stable static localized structures in one dimension, Phys. Rev. Lett. **84**, 3069 (2000).

[14] P. Coullet, C. Riera, and C. Tresser, A new approach to data storage using localized structures, Chaos **14**, 193 (2004).

[15] J. Mallet-Paret and R. D. Nussbaum, Global continuation and asymptotic behaviour for periodic solutions of a differential-delay equation, Annali di matematica pura ed applicata **145**, 33 (1986).

[16] M. Nizette, Front dynamics in a delayed-feedback system with external forcing, Physica (Amsterdam) **183D**, 220 (2003).

[17] F. Leo, S. Coen, P. Kockaert, S. P. Gorza, P. Emplit, and M. Haelterman, Temporal cavity solitons in one-dimensional kerr media as bits in an all-optical buffer, Nat. Photonics **4**, 471 (2010).

[18] M. Tlidi and L. Gelens, High-order dispersion stabilizes dark dissipative solitons in all-fiber cavities, Opt. Lett. **35**, 306 (2010).

[19] M. Tlidi, L. Bahloul, L. Cherbi, A. Hariz, and S. Coulibaly, Drift of dark cavity solitons in a photonic-crystal fiber resonator, Phys. Rev. A **88**, 035802 (2013).

[20] T. Herr, V. Brasch, J. D. Jost, C. Y. Wang, N. M. Kondratiev, M. L. Gorodetsky, and T. J. Kippenberg, Temporal solitons in optical microresonators, Nat. Photonics **8**, 145 (2014).

[21] M. Marconi, J. Javaloyes, S. Balle, and M. Giudici, How lasing localized structures evolve out of passive mode locking, Phys. Rev. Lett. **112**, 223901 (2014).

[22] M. Marconi, J. Javaloyes, S. Balle, and M. Giudici, Passive mode-locking and tilted waves in broad-area vertical-cavity surface-emitting lasers, IEEE J. Sel. Top. Quantum Electron. **21**, 85 (2015).

[23] B. Garbin, J. Javaloyes, G. Tissoni, and S. Barland, Topological solitons as addressable phase bits in a driven laser, Nat. Commun. **6**, 5915 (2015).

[24] N. N. Rosanov and G. V. Khodova, Diffractive autosolitons in nonlinear interferometers, J. Opt. Soc. Am. B **7**, 1057 (1990).

[25] M. Tlidi, P. Mandel, and R. Lefever, Localized structures and localized patterns in optical bistability, Phys. Rev. Lett. **73**, 640 (1994).

[26] W. J. Firth and A. J. Scroggie, Optical bullet holes: Robust controllable localized states of a nonlinear cavity, Phys. Rev. Lett. **76**, 1623 (1996).

[27] S. Barland, J. R. Tredicce, M. Brambilla, L. A. Lugiato, S. Balle, M. Giudici, T. Maggipinto, L. Spinelli, G. Tissoni, T. Knödl, M. Miller, and R. Jäger, Cavity solitons as pixels in semiconductor microcavities, Nature (London) **419**, 699 (2002).

[28] P. Genevet, S. Barland, M. Giudici, and J. R. Tredicce, Cavity soliton laser based on mutually coupled

semiconductor microresonators, Phys. Rev. Lett. **101**, 123905 (2008).

[29] Y. Tanguy, T. Ackemann, W. J. Firth, and R. Jäger, Realization of a semiconductor-based cavity soliton laser, Phys. Rev. Lett. **100**, 013907 (2008).

[30] F. Pedaci, G. Tissoni, S. Barland, M. Giudici, and J. R. Tredicce, Mapping local defects of extended media using localized structures, Appl. Phys. Lett. **93**, 111104 (2008).

[31] T. Ackemann, N. Radwell, Y. Noblet, and R. Jäger, Disorder mapping in VCSELs using frequency-selective feedback, Opt. Lett. **37**, 1079 (2012).

[32] F. T. Arecchi, G. Giacomelli, A. Lapucci, and R. Meucci, Two-dimensional representation of a delayed dynamical system, Phys. Rev. A **45**, R4225 (1992).

[33] G. Giacomelli and A. Politi, Relationship between delayed and spatially extended dynamical systems, Phys. Rev. Lett. **76**, 2686 (1996).

[34] S. A. Kashchenko, Zh. Vychisl. Mat. Mat. Fiz. **38**, 457 (1998) [The Ginzburg-Landau equation as a normal form for a second-order difference-differential equation with a large delay, Comput. Math. Math. Phys. **38**, 443 (1998)].

[35] G. Giacomelli, F. Marino, M. A. Zaks, and S. Yanchuk, Coarsening in a bistable system with long-delayed feedback, Europhys. Lett. **99**, 58005 (2012).

[36] G. Giacomelli, F. Marino, M. A. Zaks, and S. Yanchuk, 'Nucleation in bistable dynamical systems with long delay, Phys. Rev. E **88**, 062920 (2013).

[37] F. Marino, G. Giacomelli, and S. Barland, Front pinning and localized states analogues in long-delayed bistable systems, Phys. Rev. Lett. **112**, 103901 (2014).

[38] M. Nizette, Stability of square oscillations in a delayed-feedback system, Phys. Rev. E **70**, 056204 (2004).

[39] A. Gavrielides, T. Erneux, D. W. Sukow, G. Burner, T. McLachlan, J. Miller, and J. Amonette, Square-wave self-modulation in diode lasers with polarization-rotated optical feedback, Opt. Lett. **31**, 2006 (2006).

[40] J. Mulet, M. Giudici, J. Javaloyes, and S. Balle, Square-wave switching by crossed-polarization gain modulation in vertical-cavity semiconductor lasers, Phys. Rev. A **76**, 043801 (2007).

[41] L. Weicker, T. Erneux, O. D'Huys, J. Danckaert, M. Jacquot, Y. Chembo, and L. Larger, Strongly asymmetric square waves in a time-delayed system, Phys. Rev. E **86**, 055201 (2012).

[42] S. Yanchuk, L. Lücken, M. Wolfrum, and A. Mielke, Spectrum and amplitude equations for scalar delay-differential equations with large delay, Discrete Contin. Dyn. Syst. **35**, 537 (2015).

[43] P. Coullet, Localized patterns and fronts in nonequilibrium systems, Int. J. Bifurcation Chaos Appl. Sci. Eng. **12**, 2445 (2002).

[44] M. Wolfrum and S. Yanchuk, Eckhaus instability in systems with large delay, Phys. Rev. Lett. **96**, 220201 (2006).

[45] M. Nizette, T. Erneux, A. Gavrielides, and V. Kovanis, Averaged equations for injection locked semiconductor lasers, Physica (Amsterdam) **161D**, 220 (2002).